Sādhanā (2024)49:5
https://doi.org/10.1007/s12046-023-02347-1

Effect of multiple protrusions on thermal performance of jet impingement with smooth concave surface

JAYKUMAR JOSHI*, AKHALESH SHARMA, PAWAN SHARMA and SANTOSH K SAHU

Department of Mechanical Engineering, Indian Institute of Technology, Indore 453 552, India
e-mail: phd1901103002@iiti.ac.in

MS received 19 April 2023; revised 3 October 2023; accepted 18 October 2023

Abstract. The current study uses numerical methods to evaluate the thermal and flow characteristics of air jet impingement on concave multi-protruded surfaces. A two-dimensional numerical analysis is carried out with the help of commercially available FLUENT package. The impact of different geometric parameters is studied, including protrusion shape (convex and triangle), protrusion height and central angle by protrusions (α). Multiple protrusions on a surface lead to a series of peaks and valleys in the local *Nu* variation, which governs the overall thermal performance of jet impingement. It is found that protrusions with lower central angle by protrusions improve the heat transfer attributes compared to smooth surface, irrespective of protrusion size and shape. A drastic improvement in thermal performance is noted by replacing convex protrusion with triangle protrusion, particularly at the larger central angle by protrusions (α).

Keywords. Convex protrusions; concave surface; jet impingement; multiple protrusions; numerical.

1. Introduction

Jet impingement cooling is used in various industrial areas due to its superior cooling rate for different thermal applications, including cooling aircraft components, metal processing, and textile industry [1, 2]. Over the years, different studies have been conducted to understand the flow and thermal attributes of jet impingement for cooling applications. Although most of the studies are related to the flat surface, very few studies are conducted to analyse the effect of surface curvature. The surface curvature greatly affects the boundary layer formation and thermal characteristics of jet impingement [3, 4] and leads to improvement or deterioration in the heat transfer behaviour of jet impingement [5]. Introducing surface roughness, ribs, protrusions and dimples is a passive cooling method to improve the thermal behaviour of jet impingement [6].

The impact of roughness or pattern on a flat surface with jet impingement cooling is also studied through various experimental and numerical investigations. Zhang *et al* [7] have observed an improvement in the higher heat transfer compared to the smooth surface by generating a single convex protrusion on a surface. Bolek and Bayratkar [8] studied the impact of single protrusion on a local Nusselt number distribution. It was found that rectangular and convex protrusions improve thermal performance in the stagnation and wall jet regions, respectively. Gau and Lee [9] carried out the flow visualisation study to understand the flow patterns of jet impingement on rib roughened wall; the study revealed that recirculation zone is formed between the protrusions of the rib roughness, acting as a barrier that hindered the penetration of the jet into the cavities formed by the ribs on the wall. Gau and Lee [10] analysed the effect of different protrusion shapes and pitches on the flow behaviour; the larger pitch ratio and triangle protrusion enhance the penetration of jet between protrusions compared to smaller pitch ratio and rectangular protrusions. Dobbertean and Rahman [11] have reported similar observations with triangle ribs. Sagot *et al* [12] have noted a significant improvement in the local heat transfer with square and triangle grooves at smaller nozzle to plate distance. Most of the previous studies are limited to the flat surface in conjunction with various protrusion arrangements on a surface. However, only a small number of studies have investigated the applicability of protrusions on a concave surface.

Hadipour *et al* [13] studied the effect of single triangle protrusion on local heat transfer performance; the authors reported the enhancement in the thermal performance by introducing a triangle rib in the stagnation zone during two-dimensional jet impingement on a concave surface. Studies have also been done to find the optimal location of a single convex protrusion with a concave surface [14]. It is reported that the location of single protrusion has less impact on the overall heat transfer behaviour; however, multiple protrusions on a surface can boost thermal performance up to 8% for a curved surface [14]. Previous studies have found that when jet impinges on a protruded

*For correspondence
Published online: 19 December 2023

surface, two new phenomena are observed such as reattachment of flow and formation of recirculation zone, which improves and deteriorates the thermal performance, respectively. Flow separation is observed at the edge of protrusion due to the adverse pressure gradient, which leads to the formation of recirculation zone. A study on multiple protrusions suggests that the distance between protrusions can increase or decrease the overall thermal performance by 15–20% [4]. However, no thorough investigation has been conducted to analyse the cause and impact of recirculation zone for jet impingement cooling. The present study aims to analyse the effect of protrusion shape and its arrangement on the flow behaviour and thermal performance of jet impingement. A thorough investigation is conducted to analyse the impact of different multiple protrusion arrangements by varying the protrusion shape, height and central angle by protrusions.

2. Computational methodology

This section includes the physical domain, computational domain, governing equations, boundary conditions, numerical model, and assumptions for the present study. The details are elaborated below.

2.1 *Physical and computational domain*

The physical geometry and the computational zone for the present investigation are described in figures 1(a) and (b), respectively. Here, a two-dimensional slot nozzle is used with nozzle width (B) of 5 mm and curvature ratio (B/D) of 0.033; these conditions are consistent with different industrial applications, including various aircraft components [15] and remained constant for the present study. A detailed description of operating conditions and assumptions for the simulation are described in the upcoming section.

2.2 *Geometric and operational parameters*

A non-confined slot jet impingement cooling is studied in the present investigation. This study analyses different geometric and operating parameters, including Reynolds number (Re = 5000–15000), protrusion shape (convex, triangle), protrusion height and central angle by protrusions (α) at H/B = 6. To ensure consistency, a standardised naming convention is adopted, denoted as $X_1N_1PN_2AN_3$, where N1, N2, and N3 represent the height (a), central angle by protrusions (α), and protrusion angle (θ) of the protrusions, respectively as shown in figure 2. Central angle by protrusion (α) indicates the angle subtended by two adjacent protrusions at the centre of the curves surface as illustrated in figure 2(a). The protrusion angle (θ) is the tip or vertex angle formed by the two sides of the triangle that intersect at the vertex or corner of the triangle as shown in figure 2(b). For a convex protrusion, the protrusion height will be the same as protrusion radius, and for a triangle protrusion, triangle height will be the same as the protrusion height. For a convex protrusion, the protrusion angle value (θ) is not needed. The numerical values for N_1, N_2, and N_3 range from 1.25 to 5 mm, 2.5° to 10°, and 90° to 150°, respectively. The letter X_1 indicates the shape of the protrusion, where "D" and "T" representing convex and

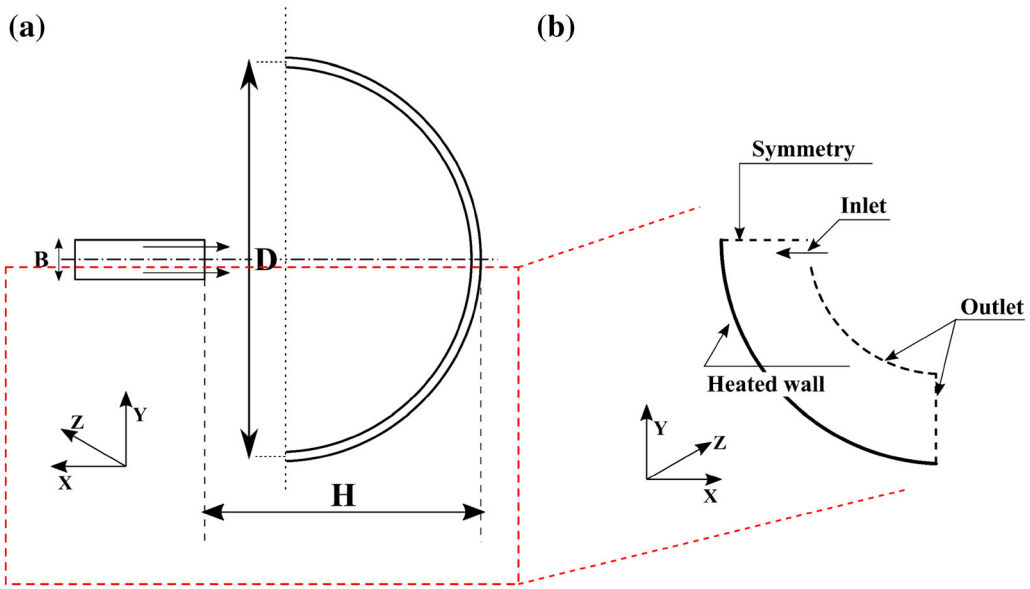

Figure 1. A simplified (**a**) physical domain and (**b**) computational domain of the present study.

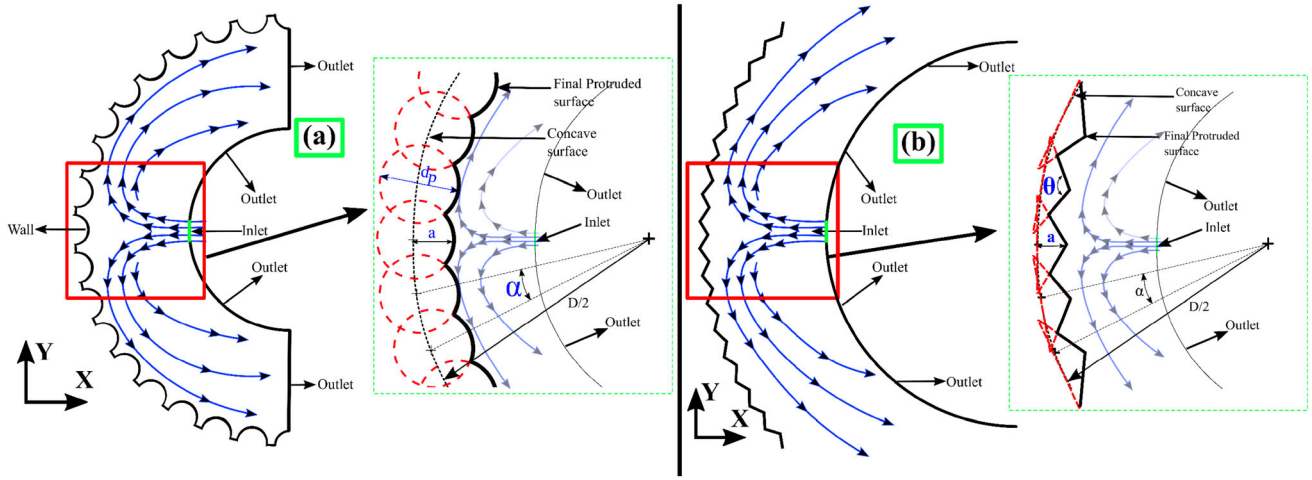

Figure 2. Schematic diagram of protruded concave surface with (**a**) convex and (**b**) triangle protrusions.

triangular protrusions, respectively. For example, "T2.5P5A150" represents a triangular protrusion with a height of 2.5 mm, $\alpha = 5°$, and $\theta = 150°$, and "D2.5P5" represents a convex protrusion with a protrusion height of 2.5 mm and $\alpha = 5°$.

2.3 *Mathematical modelling*

Details about the different governing equations and assumptions for the present study are listed below:

(1) The end wall effect is neglected in the simulation, and a two-dimensional numerical simulation is carried out in the present investigation.
(2) Fluid properties are constant throughout the domain.
(3) The working fluid is incompressible.

i. Continuity Equation

$$\frac{\partial U_i}{\partial x_i} = 0 \tag{1}$$

ii. Momentum Equation

$$U_j \frac{\partial U_i}{\partial x_j} = -\frac{1}{\rho}\frac{\partial P}{\partial x_i} + \frac{\partial}{\partial x_i}\left[\nu\left(\frac{\partial U_i}{\partial x_j}\right) - \overline{u_i' u_j'}\right] \tag{2}$$

iii. Energy Equation

$$U_i \frac{\partial T}{\partial x_j} = \frac{\partial}{\partial x_i}\left(\frac{k_f}{\rho C_p}\frac{\partial T}{\partial x_i} - \overline{u_i' T'}\right) \tag{3}$$

where ρ, ν, U_i, P, T, k_f, C_p Indicates density, kinetic viscosity, velocity, pressure, temperature, thermal conductivity of fluid and specific heat capacity of fluid, respectively. Here u_i' and T' indicates the fluctuating components of velocity and temperature, respectively. The Reynolds stresses, $-\overline{u_i' u_j'}$ are estimated based on the Boussinesq hypothesis.

- Inlet boundary:
  u = Constant, $v = 0$; Turbulence Intensity = 5% & Turbulence viscosity ratio = 10
- Constant heat flux boundary

$$q'' = -k_f \frac{\partial T}{\partial n} = 5000 \text{ W/m}^2, \quad u = v = 0$$

  where n indicates the direction normal to the surface.
- Pressure outlet
  P_{ext} = 1 atm

$$\frac{\partial T}{\partial n} = \frac{\partial k}{\partial n} = \frac{\partial \epsilon}{\partial n} = 0$$

The pressure-velocity coupling is done with the coupled algorithm. A second-order upwind scheme is used for discretizing the pressure, momentum, turbulence kinetic energy, and specific dissipation rate equations. The convergence criteria are set as 1×10^{-5} for all the equations except energy (1×10^{-8}).

2.4 *Computational methodology*

A commercially available CFD code FLUENT is used in the present investigation to perform the different simulations. A RANS (Reynolds-Averaged Navier Stokes) equation-based turbulent model is used in the present investigation. An *SST k-ω* Turbulent model is chosen based on previous studies for jet impingement cooling. It gives comparatively better results compared to the *k-ε* model. The SST k-ω model undergoes a shift in its behavior to a k-ε model when it is located far away from the wall. This transition in models leads to a decrease in the sensitivity of the inlet condition. Additionally, it has demonstrated superior performance in adverse pressure gradients near the

intended surfaces, making it particularly suitable for the stagnation zone [16]. This turbulence model solved two equations involving turbulence kinetic energy (k) and a specific dissipation rate (ω). The equation for the same is written below:

$$\frac{\partial(\rho k u)}{\partial x} = \frac{\partial}{\partial x}\left(\Gamma_k \frac{\partial k}{\partial x}\right) + G_k - Y_k \tag{4}$$

$$\frac{\partial(\rho \omega u)}{\partial x} = \frac{\partial}{\partial x}\left(\Gamma_\omega \frac{\partial \omega}{\partial x}\right) + G_\omega - Y_\omega + D_\omega \tag{5}$$

where G_k, G_ω indicates the turbulence kinetic energy production and generation of specific dissipation rate, respectively. Here, Γ_k and Γ_ω denotes the effective diffusivity of turbulence kinetic energy and specific dissipation rate, respectively. while D_ω Indicate the cross-diffusion term. The corresponding expressions for Γ_k and Γ_ω is represented below. respectively,

$$\Gamma_k = \mu + \frac{\mu_t}{\sigma_k} \tag{6}$$

$$\Gamma_\omega = \mu + \frac{\mu_t}{\sigma_\omega} \tag{7}$$

where σ_k and σ_ω denotes the turbulent Prandtl number, for turbulence kinetic energy and specific dissipation rate, respectively, while μ_t and μ indicates the turbulence viscosity and fluid dynamics viscosity, respectively.

$$G_k = -\overline{\rho u' v'}\frac{\partial v}{\partial x} \tag{8}$$

$$G_\omega = \frac{\alpha}{v_t} G_k \tag{9}$$

The expression for Y_k and Y_ω are elaborated below.

$$Y_k = \rho \beta^* k \omega \tag{10}$$

$$Y_\omega = \rho \beta \omega^2 \tag{11}$$

where α, β^*, and β denote the coefficients and v_t indicates the kinematic turbulence viscosity.

2.5 *Data reduction*

The Reynolds number is calculated at the nozzle exit according to the fluid velocity at the nozzle exit and expressed as [17]:

$$Re = \frac{\rho u d_h}{\mu} \tag{12}$$

here u, d_h, ρ and μ denotes the fluid velocity, hydraulic diameter of nozzle, density and viscosity of fluid, respectively. The hydraulic diameter for the slot jet is defined as below:

$$d_h = \frac{4A}{p}; d_h \approx 2B \tag{13}$$

where A and p denotes the cross-section of nozzle and perimeter of the nozzle, respectively. The heat transfer coefficient h is defined according to Newton's law of cooling as

$$h_i = \frac{q''}{T_j - T_w} \tag{14}$$

where T_j, T_w and q'' denote the jet temperature at the nozzle exit, wall temperature and imposed constant heat flux condition at the wall, respectively. The Nusselt number and heat transfer coefficient is defined as

$$h_{avg} = \int_{-D/2}^{D/2} h_i . dy \tag{15}$$

$$Nu_{avg} = \frac{h_{avg} d_h}{k_f} \tag{16}$$

where k_f denotes the thermal conductivity of air. The average Nusselt number and h_{avg} is calculated as [18]. Thermal performance of jet on a multi-protruded surface is analysed by normalised Nu and is calculated as

$$Nu_{Norm} = {}^{Nu_{protruded}}/_{Nu_{smooth}} \tag{17}$$

where $Nu_{protruded}$ and Nu_{smooth} represents the overall Nu with a multi-protruded surface and smooth surface, respectively.

2.6 *Grid independence study*

In the present investigation, the computational domain is divided into numerous small finite volumes with an unstructured grid system involving high grid density near the wall zone. To ensure the accuracy of the simulation, it is crucial to perform a grid independence investigation to identify the optimal and suitable meshing. Various mesh arrangements were studied by maintaining a constant y^+ value based on the local Nu variation, as depicted in figure 3(a). It displays the local Nu variation for cell sizes ranging from 0.25 mm (Elements no. = 50725) to 0.5 mm (Elements no. = 14400). Although a slight deviation in the local Nu variation was observed in the stagnation zone, there were no changes in Nu variation in the wall-jet region. The maximum size of each cell is limited to 0.35 mm (Elements no. = 27325) in the present investigation, and an inflation layer is generated to attain high grid density near the heated wall. Fifteen inflation layers are generated near the wall and the first layer thickness of the inflation layer is created in such a way that the y^+ value near the heated will not exceed the unity value.

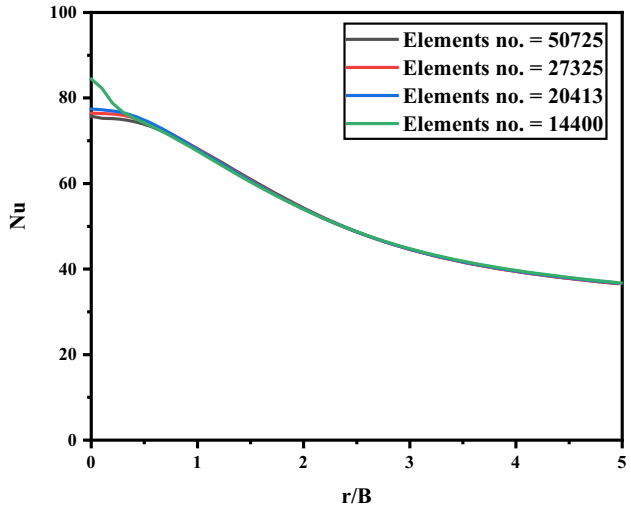

Figure 3. Shows the local *Nu* variation for slot jet impingement on a concave surface at *Re* = 10000, *B/D* = 0.033 and *H/B* = 6 for various computational grids.

2.7 *Validation*

It is worth noting that experimental data for a protruded concave surface is rare in existing literature. To address this, the present computational results are validated against concave smooth surfaces, as depicted in figure 4. The overall Nusselt number distribution of slot jet impingement on a concave surface is validated using past data by Sharif and Mothe [19] for a range of Reynolds numbers, as shown in figure 4(a). The validation results show good agreement with a deviation of only 1.5%. Additionally, the local Nusselt number distribution of slot jet impingement on a concave smooth surface is compared with the past data of Choi *et al* [20] at *H/B* = 4 and *Re* = 4740, and the results show good agreement with an average deviation of 15%, as shown in figure 4(b).

3. Results and discussion

In the present study, the thermal performance of smooth and multi-protruded surfaces is studied concerning local and average *Nu*. The fluid dynamics of jet impingement is analysed with the help of pressure contours and streamlines for smooth and multi-protruded surfaces.

3.1 *Effect of protrusion height and central angle by protrusion (α)*

Figure 5 illustrates the variation of local Nusselt number (*Nu)* on smooth and multi-protruded surfaces at *Re* = 15000, with different protrusion heights ranging from 2.5 to 5 mm and central angle by protrusion (α) varying from 2.5° to 10°. In figure 5(a), a comparison is made between the local *Nu* variation on smooth and multi-protruded surfaces (D2.5P10). On a smooth surface, a continuous decrease in local *Nu* is observed as we move away from the stagnation zone, which can be divided into stagnation and wall-jet zones. However, a series of peaks and valleys in the heat transfer are observed with a multi-protruded surface. Previous studies have suggested that the recirculation zone traps fluid in a localised zone, increasing fluid temperature and decreasing heat transfer (valley region). A reattachment of flow with the surface restarts the boundary layer formation on the surface, resulting in peaks in the local heat transfer distribution [21]. The flow motion can be divided into various zones: stagnation zone, recirculation zone (valley region), reattachment of flow (peak region), and

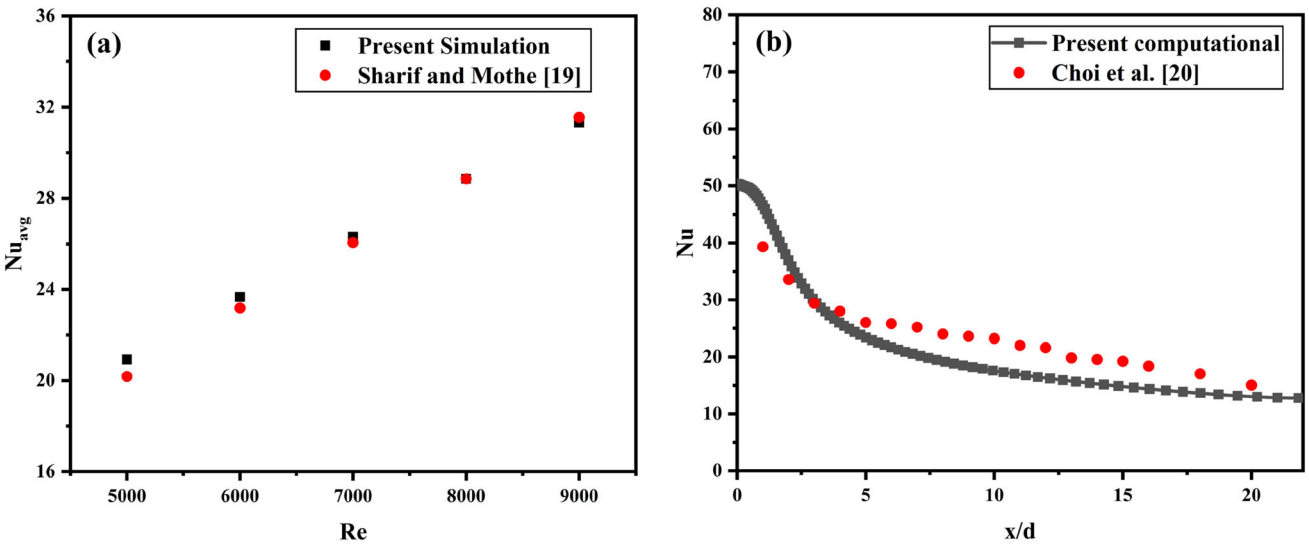

Figure 4. A comparison of present investigation with previous investigations (**a**) average *Nu* at various *Re* at *H/B* = 4. (**b**) Local *Nu* distribution of present study with past data for a concave surface at *Re* = 4740 at *H/B* = 4 and *B/D* = 0.033.

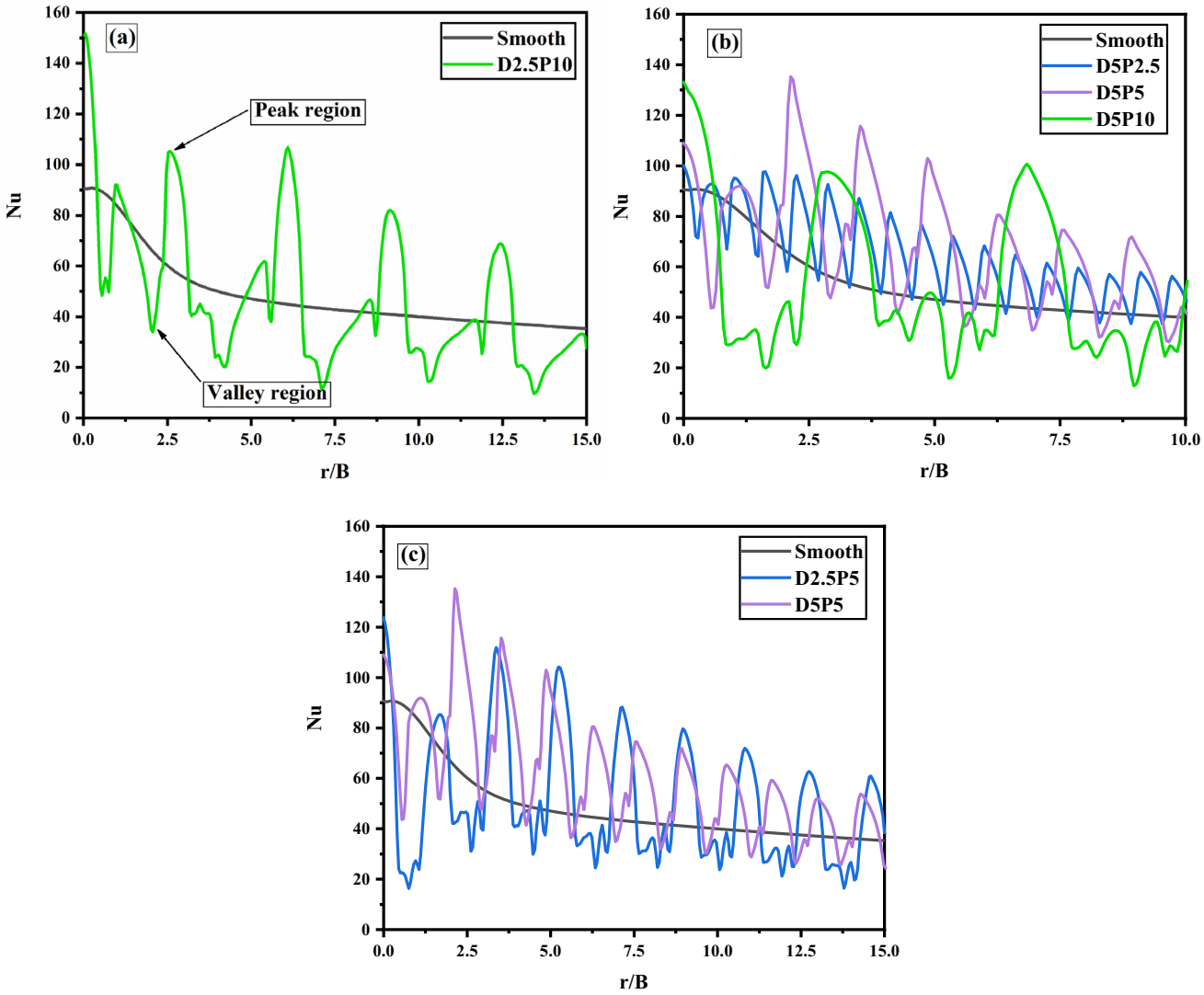

Figure 5. Local *Nu* variation for smooth and multi-protruded surface at *Re* = 15000 at *H/B* = 6.

wall-jet zone. The formation of these zones depends on the geometry and size of the protrusion, and the dominance of these zones determines the enhancement or deterioration in the overall thermal performance with the protruded surface.

A larger value of central angle by protrusion *(α)* results in a larger valley region with identical protrusion height as shown in figure 5(b). The distance between protrusions increases as the central angle by protrusion (α) increases, creating a larger valley region. Furthermore, the minimum value of *Nu* in the valley region also decreases with an increase in the value of central angle *(α)*. As the value of central angle by protrusion *(α)* decreases from D5P10 to D5P2.5, a significant reduction in the size of valley region is observed. Furthermore, the increased number of protrusions on the surface leads to more spikes in the local *Nu* distribution, which positively impacts the thermal performance of jet impingement.

Figure 5(c) presents the influence of protrusion height on the local *Nu* distribution. A noticeable change is observed in the valley region compared to the peak region when the protrusion height is decreased. A decrease in protrusion height at an identical value of central angle by protrusion *(α)* results in a larger valley region, which negatively impacts the overall thermal performance. Conversely, higher heat transfer behaviour is observed in most of the wall region when using larger protrusion (D5P5) heights compared to a smooth surface. The study reveals that larger protrusions and smaller central angle (D5P2.5) by protrusion lead to a smaller valley region and a large number of spikes in the local *Nu*, which improves heat transfer.

Figure 6 illustrates the streamline and pressure contours for both smooth and multi-protruded surfaces. On a smooth surface, a continuous flow of air parallel to the surface is observed in the wall-jet region. However, on a multi-

protruded surface, a series of recirculation zone and reattachment of flow is observed. The size of the recirculation zone varies depending on the protrusion size and central angle by protrusion (α). The presence of protrusions also results in peaks in the pressure contours due to the reattachment of flow on the surface. A significant reduction in the size of the recirculation zone is observed with increasing protrusion height for D2.5P5 to D5P5, which positively impacts the local *Nu* variation as previously shown. Similar effects are noted with a decrease in the value of central angle of protrusion *(α)* for D5P10 to D5P2.5. An increase in central angle by protrusion (α) lead to flow separation from the surface, generating adverse pressure gradients at the end of protrusions and deteriorating heat transfer, as reported in [7].

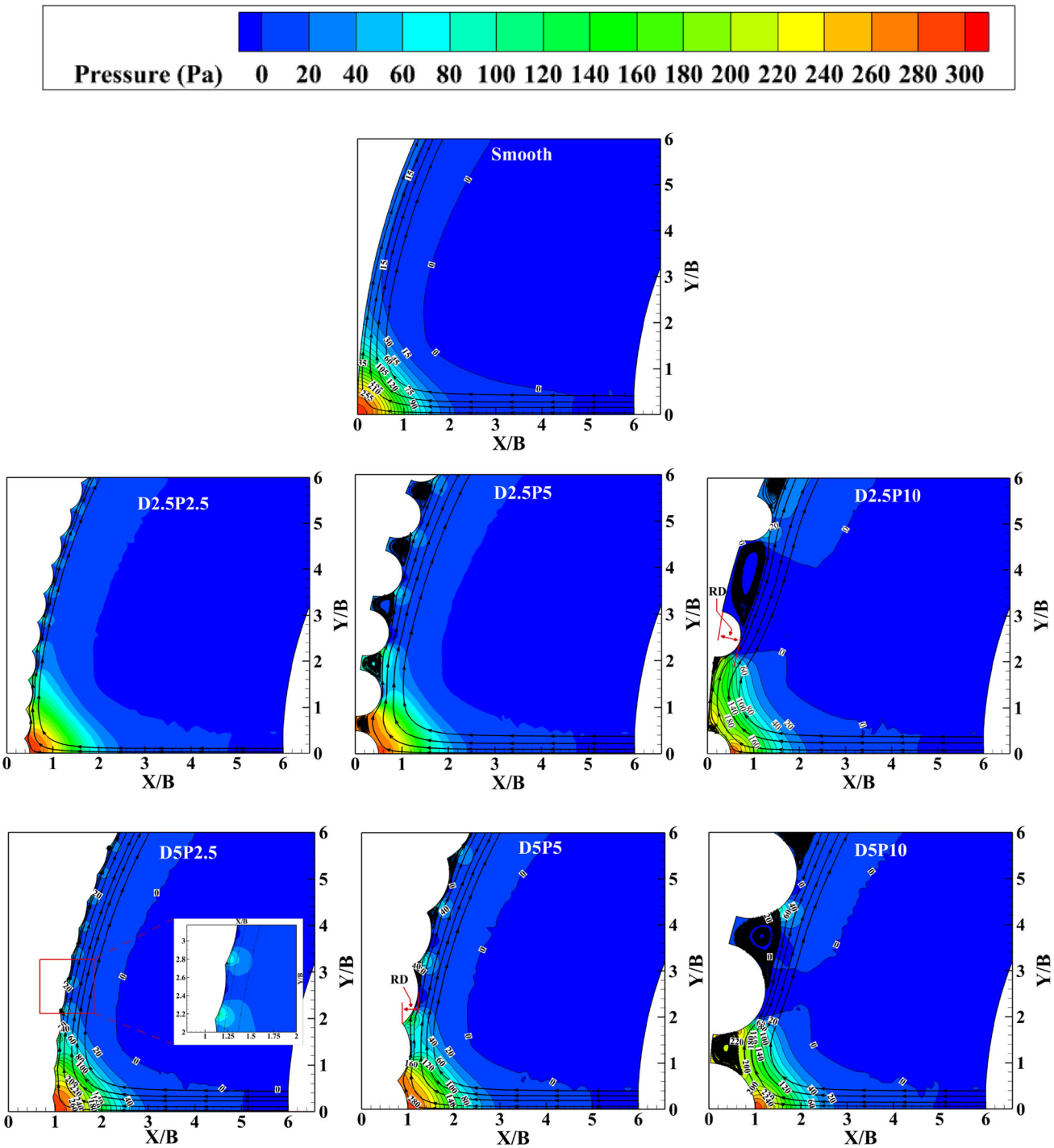

Figure 6. Streamline and pressure contours for a smooth and multi-protruded surface at *Re* = 15000 and *H/B* = 6.

Figure 7 presents the impact of central angle by protrusion *(α)* (figure 7a) and protrusion height (figure 7b) on the overall *Nu* variation. A connection between the streamline diagram (figure 6) and heat transfer performance (figure 7) is observed. Multi-protruded surface with larger circulation zone such as D5P10 leads to a decrease in thermal performance when compared to a smooth surface. Conversely, all multi-protruded surfaces with smaller recirculation zones, such as D5P5, D5P2.5, D2.5P2.5, and D5P2.5, exhibit higher thermal performance than the smooth surface. It is worth noting that when the central angle with protrusion (α) is lower, the recirculation zone becomes smaller and the overall Nusselt number increases, regardless of the size of the protrusion. The findings indicate that a multi-protruded surface with higher value of protrusion height and a lower value of central angle by protrusion (α) leads to an enhancement in the overall thermal performance of jet impingement.

3.2 *Effect of protrusion shape*

Figure 8 illustrates a comparison of streamline contours for a multi-protruded surface with convex and triangle-shaped protrusions, where the central angle by protrusion (α) and protrusion height are kept identical, while the protrusion angle (θ) is varied from 90° to 150° to investigate its impact on flow dynamics. For θ = 90°, a large recirculation zone forms between the protrusions due to the lower penetration of the jet, hindering heat transfer performance. However, as protrusion angle increases, the size of the recirculation zone reduces. Moreover, an increase in protrusion angle leads to a decrease in the relative distance (*RD*) between the peak and valley of protrusions on the surface, resulting in improved jet penetration between the protrusions. This implies that the protrusion angle plays a significant role in determining the fluid motion on the surface.

Figure 9 demonstrates the influence of protrusion angle on the overall thermal performance of jet impingement with convex protrusions while keeping the protrusion height and central angle by protrusion (α) identical. In the case of triangle protrusions, a significant change in the overall *Nu* (upto 34%) is observed as the protrusion angle is varied from 90° to 150°, at a consistent value of central angel by protrusion (α*)* and protrusion height. Streamline contours for both cases (θ = 90°, 150°) indicate a larger reduction in the recirculation zone with higher protrusion angles, leading to improved heat transfer performance in jet impingement. The study suggests that a smaller value of α positively impacts heat transfer, regardless of protrusion size, due to a smaller recirculation zone and a larger number of peaks in the local *Nu* variation. Furthermore, it is found that triangle protrusions can be used with a larger value of central angel by protrusion (α*)* to enhance thermal performance, as compared to convex protrusions, which reduce the number of indentations on the surface.

4. Conclusion

The present investigation focuses on the thermal performance of jet impingement on a multi-protruded surface and analyse the effect on protrusion shape, protrusion height and central angle by protrusion (α) on a local and overall heat transfer characteristics of jet impingement.

1. A series of peak and valley in the local *Nu* variation is observed by introducing the protrusion on the surface.

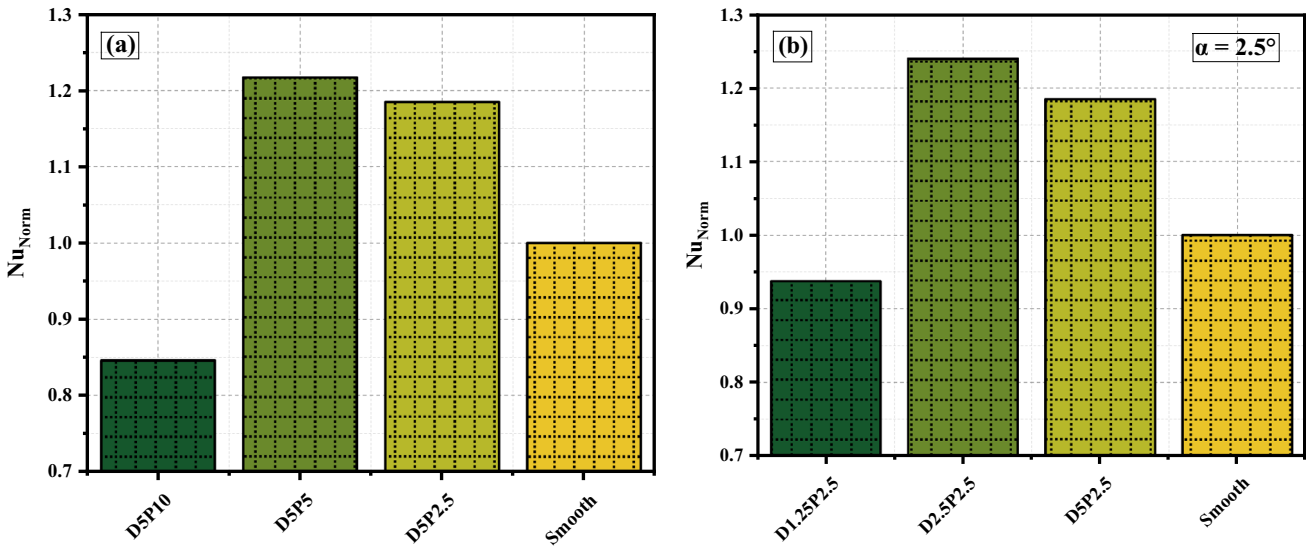

Figure 7. Normalised *Nu* variation for smooth and multi-protruded with convex protrusion surfaces at Re = 15000.

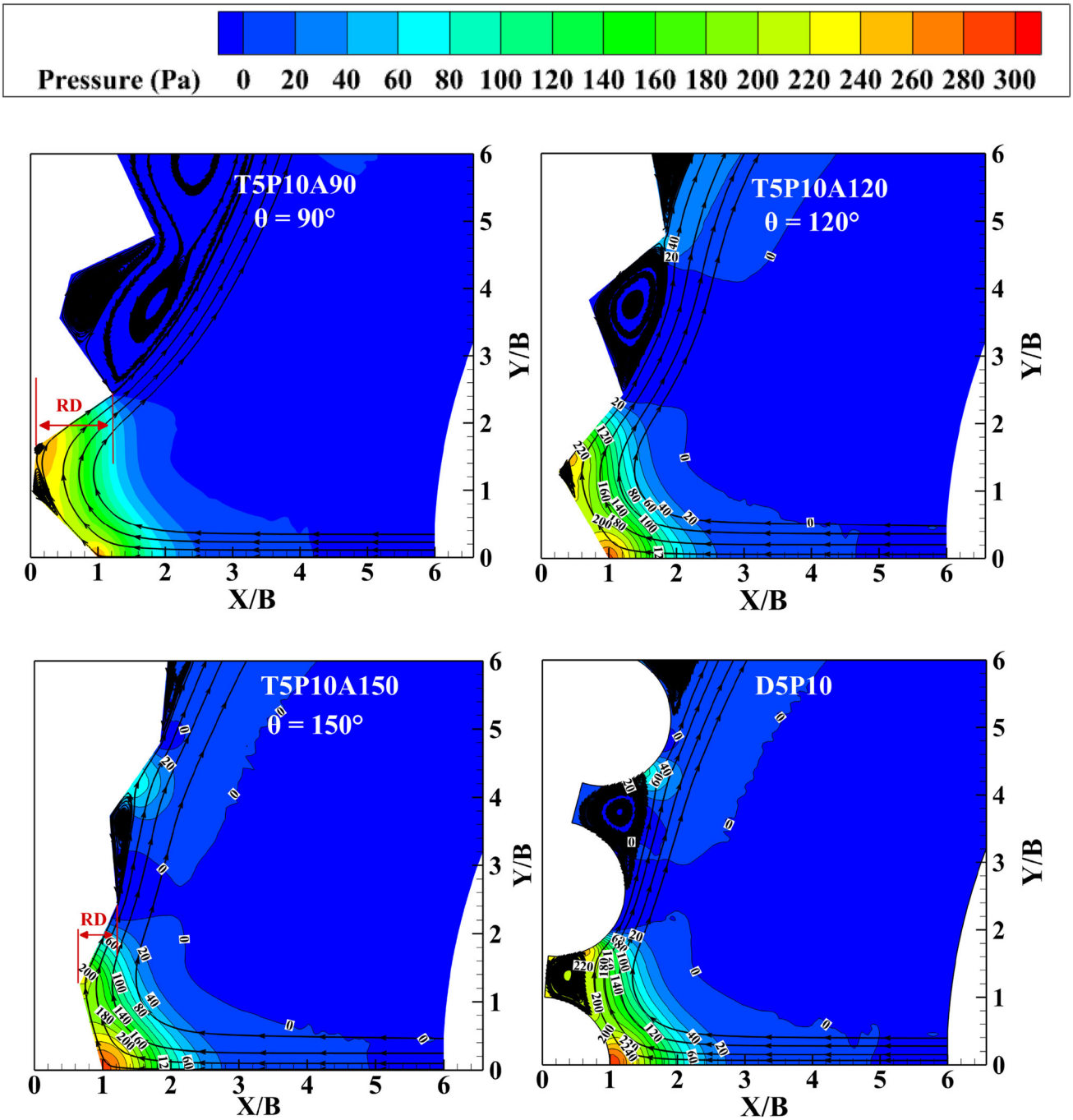

Figure 8. Streamline and pressure contours for multi-protruded surfaces at Re = 15000 with a = 5 mm and α = 10°.

2. It is found out that the protrusion with a lower value of central angel by protrusion (α) improves the thermal performance compared to the smooth surface, irrespective of the protrusion size and protrusion shape.
3. With an increase in the protrusion height, an improvement in the overall thermal performance of jet impingement is noted.
4. A peak in the *Nu* is noted with all the configurations; however, the size of the recirculation zone has much impact on the local heat transfer characteristics of jet impingement.
5. A reduction in the size of recirculation zone is observed by increasing the protrusion angle, which leads to improvement in the heat transfer performance. An arrangement of triangle protrusion with a larger value of central angle by protrusion (α) can be used to improve the thermal performance of jet impingement, reducing the number of indentations on the surface.

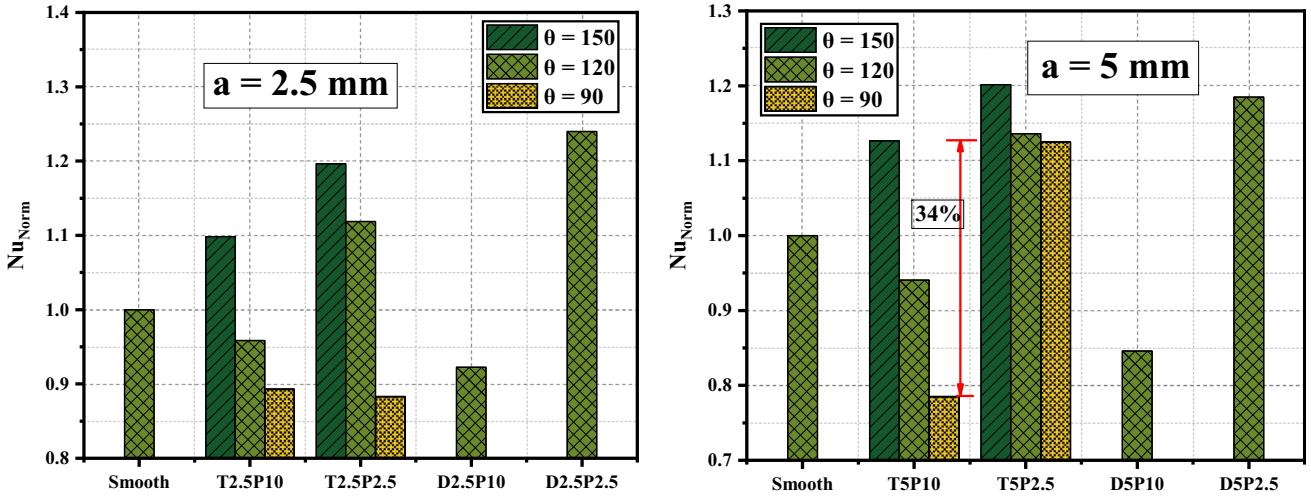

Figure 9. Normalised *Nu* variation for smooth and multi-protruded surfaces for triangle and convex protrusion surface at *Re* = 15000.

List of symbols

a	Height of protrusion, mm
B	Width of nozzle, mm
B/D	Curvature ratio
C_p	Specific heat capacity of air, J kg^{-1} K^{-1}
d_h	Hydraulic diameter of nozzle, mm
d_p	Protrusion diameter, mm
H/B	Non-dimensionless nozzle-to-plate distance
h	Heat transfer coefficient, Wm^{-2} K^{-1}
Nu	Nusselt number
q''	Constant heat flux, W m^{-2}
r	Length on surface from the stagnation point, mm
T_i	Temperature of jet, K
T_w	Wall temperature, K

Greek symbols

α	Angle subtended by two adjacent protrusions at the centre of the curves surface (°)
θ	Protrusion angle (°)

Subscripts

avg	Average
j	Jet
Norm	Normalized

References

[1] Sharma A K, Lodhi U K, Kumar G and Sahu S K 2019 Effect of jet inclination and coolant flow rate on thermal and rewetting behavior during bottom jet impingement on hot horizontal surfaces. *Steel Res. Int.* 90(10): 1900171

[2] Sharma A K and Sahu S K 2019 The thermal and rewetting behavior of hot moving surface by water jet impingement. *Appl. Therm. Eng.* 159: 113950

[3] Fenot M, Vullierme J J and Dorignac E 2005 Local heat transfer due to several configurations of circular air jets impinging on a flat plate with and without semi-confinement. *Int. J. Therm. Sci.* 44(7): 665–675

[4] Joshi J and Sahu S K 2023 Effect of single and multiple protrusions on thermal performance of slot jet impingement with curved surface. *Appl. Therm. Eng.* 230: 120757

[5] Joshi J and Sahu S K 2022 Heat transfer characteristics of flat and concave surfaces by circular and elliptical jet impingement. *Exp. Heat Transf.* 35(7): 938–963

[6] Hsieh S S, Tsai H H and Chan S C 2004 Local heat transfer in rotating square-rib-roughened and smooth channels with jet impingement. *Int. J. Heat Mass Transf.* 47(12–13): 2769–2784

[7] Zhang D, Qu H, Lan J, Chen J and Xie Y 2013 Flow and heat transfer characteristics of single jet impinging on protrusioned surface. *Int. J. Heat Mass Transf.* 58(1–2): 18–28

[8] Bolek A and Bayraktar S 2019 Flow and heat transfer investigation of a circular jet issuing on different types of surfaces. *Sadhana Acad. Proc. Eng. Sci.* 44(12): 242

[9] Gau C and Lee C C 1992 Impingement cooling flow structure and heat transfer along rib-roughened walls. *Int. J. Heat Mass Transf.* 35(11): 3009–3020

[10] Gau C and Lee I C 2000 Flow and impingement cooling heat transfer along triangular rib-roughened walls. *Int. J. Heat Mass Transf.* 43(24): 4405–4418

[11] Dobbertean M M and Rahman M M 2016 Numerical analysis of steady state heat transfer for jet impingement on patterned surfaces. *Appl. Therm. Eng.* 103: 481–490

[12] Sagot B, Antonini G and Buron F 2010 Enhancement of jet-to-wall heat transfer using axisymmetric grooved impinging plates. *Int. J. Therm. Sci.* 49(6): 1026–1030

[13] Hadipour A, Rajabi Zargarabadi M and Mohammadpour J 2020 Effects of a triangular guide rib on flow and heat transfer in a turbulent jet impingement on an asymmetric concave surface. *Phys. Fluids* 32(7): 075112

[14] Singh A, Chakravarthy B and Prasad B 2021 Numerical simulations and optimization of impinging jet configuration. *Int. J. Numer. Methods Heat Fluid Flow.* 31(1): 1–25

[15] Singh A and Prasad B V S S S 2019 Influence of novel equilaterally staggered jet impingement over a concave surface at fixed pumping power. *Appl. Therm. Eng.* 148: 609–619

[16] Sharif M A R and Mothe K K 2009 Evaluation of turbulence models in the prediction of heat transfer due to slot jet impingement on plane and concave surfaces. *Numer. Heat Transf. Part B Fundam.* 55(4): 273–294

[17] Singh P K, Joshi J and Sahu S K 2023 Heat transfer characteristics of the flat plate integrated with metal foam of varying thickness using an unconfined circular air-jet impingement. *Therm. Sci. Eng. Prog.* 41: 101810

[18] Rau M J and Garimella S V 2013 Local two-phase heat transfer from arrays of confined and submerged impinging jets. *Int. J. Heat Mass Transf.* 67: 487–498

[19] Sharif M A R and Mothe K K 2010 Parametric study of turbulent slot-jet impingement heat transfer from concave cylindrical surfaces. *Int. J. Therm. Sci.* 49(2): 428–442

[20] Choi M, Yoo H S, Yang G, Lee J S and Sohn D K 2000 Measurements of impinging jet flow and heat transfer on a semi-circular concave surface. *Int. J. Heat Mass Transf.* 43(10): 1811–1822

[21] Xie Y, Li P, Lan J and Zhang D 2013 Flow and heat transfer characteristics of single jet impinging on dimpled surface. *J. Heat Transfer.* 135(5): 1–15